HEFAT2014
10th International Conference on Heat Transfer, Fluid Mechanics and Thermodynamics
14 – 26 July 2014
Orlando, Florida

COMPARISON STUDY FOR FORCED CONVECTION HEAT TRANSFER OF SUPERCRITICAL CARBON DIOXIDE FLOWING IN A PIPE

Tanimizu K. and Sadr R.*
Department of Mechanical Engineering program,
Texas A&M University at Qatar,
Education City, 23874,
Doha, Qatar,

ABSTRACT

Forced convection heat transfer in supercritical carbon dioxide (SCO_2) was investigated experimentally in a horizontal circular tube with an inner diameter of 8.7 mm. The experiments were performed by varying the inlet fluid temperature, system pressure, wall heat flux, and mass flow rate. The corresponding Reynolds number at the inlet was between 20000 and 50000. Nusselt number at each section in the tube was obtained to investigate the influence of the experimental parameters on the forced convection heat transfer in the testing tube. The obtained heat transfer results were then compared with widely used empirical correlations to show their prediction accuracy for the experimental conditions tested.

INTRODUCTION

The U.S. Energy Information Administration identified Brayton cycle operating with supercritical carbon dioxide (SCO_2) as one of the major candidates for the next generation of high efficiency power plants [1]. SCO_2 Brayton cycles provide high thermal efficiency, compactness, and applicability for a wide range of thermal energy sources. Since a SCO_2 Brayton cycle is assumed to run above the critical pressure of CO_2, no phase change is expected in the cycle with availability of higher specific heat in the fluid than normal conditions. This enables application of smaller size heat exchangers [2] and elimination of condensers in the power plant [3-7] that lead to reduction of the total cost of construction. Furthermore, the peak turbine inlet temperature of the SCO_2 cycle matches with the variety of most conventional heat sources such as geothermal, coal, natural gas, and solar energy for the cycle [7]. A high efficiency power cycle may then be designed at moderate operating temperatures for such cases, e.g. efficiency of 43% at 538 ^oC and 50% at 700 ^oC are reported in the past [7].

It is necessary to understand natural/forced convection of supercritical fluids in order to be able to design the SCO_2 Brayton cycle. Forced convection of supercritical fluids such as water, carbon dioxide, nitrogen and helium in basic geometries and practical applications has been studied in the past decades. The thermal-physical properties of fluids vary significantly in the pseudocritical region, in super critical zone but close to the critical point (e.g. 31.1^oC and 73.8 bar for CO_2), even when there is a small change in temperature. The nature of the critical point, and its influence on the properties of supercritical fluids, has been discussed in the past, e.g. Carles [8]. These thermal-physical property variations help to explain the flow and heat transfer behaviors exhibited in relevant studies of supercritical CO_2 as working fluids.

Numerous researchers [9-13] studied fluid flows in pseudocritical region and proposed heat transfer correlations based on their experimental data under heating and cooling conditions for the flow. However, comparative studies of these correlations reveal that there are substantial differences in their predictions from each other [14, 15]. Pioro et al. [16] and Yoo [17], for example, provided a comprehensive review of the heat transfer characteristics of pseudocritical and supercritical fluids and discussed some suggested empirical correlations for these cases. It is evident from these studies that more experimental investigations are required in the pseudocritical region in order to develop better heat transfer correlations.

The goal of this work is to quantify the heat transfer characteristics of SCO_2 flowing in a horizontal straight pipe. Wall temperature measurements and heat transfer calculations were conducted in pseudocritical regions under heating conditions at constant heat flux cases for various inlet conditions. The obtained data is then used to evaluate performance of some existing correlations and their accuracies for the current experimental condition.

* Correspondence Author: reza.sadr@qatar.tamu.edu

NOMENCLATURE

A	[m2]	Area
Bo	[-]	Buoyancy parameter
C		Constant using in equation 1
c_p	[kJ/kg.K]	Specific heat
D	[m]	Diameter
Gr	[-]	Grashof number; $\frac{g\beta(T_w-T_b)d^3}{v_b^2}$
h	[W/m^2.K]	Heat transfer Coefficient
i	[kJ/kg]	Enthalpy
k	[W/m.K]	Thermal conductivity
L	[m]	Length
$\dot{m}$	[kg/s]	Mass flow rate
Nu	[-]	Nusselt number; $\frac{hD}{k}$
P	[bar]	Pressure
Pr	[-]	Prandtl number
q	[W/m^2]	Heat flux
Re	[-]	Reynolds number $\frac{4\dot{m}}{\pi\mu d}$
T	[K]	Temperature

Special characters

β	[1/K]	Thermal expansion
ρ	[kg/m^3]	Density
υ	[m^2/s]	kinematic viscosity
-	[-]	average

Subscripts

b	Bulk
C	Convection/Conventional
i	Inlet/Inner
m	Constant using in equation 1
out	Outlet/Outer
pc	Pseudocritical
t	Total
$t1$	Bulk or wall using in equation 1
$t2$	Bulk or wall using in equation 1
w	Wall

EXPERIMENT

Experimental set up

Figure 1 shows the schematic of the SCO2 testing facility built in Micro Scale Thermo Fluids (MSTF) laboratory at Texas A&M University at Qatar (TAMUQ). The facility was specially designed for obtaining quantitative data for thermal and dynamic behaviour near the pseudocritical region under heating conditions. The facility consists of a high pressure CO_2 supply system, a gear pump, heat exchanger (cooler), flow meter, pre-heater, tubes and valves. A CO_2 cylinder (purity 99.9%) with a dip tube, allowing liquid CO_2 to discharge from the bottom, which was connected to a helium gas cylinder to achieve the desired pressure level in the facility. Liquid CO_2 mass flow rate in the facility is kept and precisely controlled using a magnetic driven gear pump. The mass flow rate is also measured using Coriolis mass flow meters. The fluid temperature at the inlet of the test section is a key experimental parameter as it is used for calculation of the fluid properties and bulk flow temperature throughout the test section. It is controlled and adjusted to the desired value by a pre-heater which was made by the University of Wisconsin. The heating capacity of pre-heater is 5.5 kW. Several T-type thermocouple probes were installed throughout of the facility, before and after test section, to monitor the temperatures of the working fluid in the facility. Fluid pressure was measured at the test section inlet using an absolute pressure transducer with an accuracy of 0.75% (full scale). All the experimental parameters such as wall, and fluid temperatures, pressure, mass flow rate etc. were monitored by LABVIEW system.

Test section

In this study, a 1.2m long straight stainless steel tube with an inner diameter of 8.7mm was used as the test section. Eighteen K-type thermocouple probes (SCASS-040U-3, OMEGA) were installed in 65 mm intervals along the tube to measure local wall temperatures, with the first thermocouple installed 65 mm downstream from the test section inlet. The constant wall heat flux on the test section was provided by 30 electric band heaters (MBH-1215200B/120, 200W each, OMEGA) installed on the pipe outer surface. Since the band heaters are connected in the series of two and the 15 pairs are then connected in parallel, the heating capacity became 6 kW. Cylindrical copper blocks were placed between the tube and the heaters to conduct the heat flux from the heaters to the steel tube. Insulation materials were put on the outer walls of the band heaters to minimize the heat loss. The heated length of the test section is 1.14 m starting at 25 mm downstream test section inlet. The bulk fluid temperatures at both the inlet and outlet of the test section were measured using T-type thermocouple probes (HTQSS-18G-12, Omega). A differential pressure transmitter was installed in the test section to measure total pressure drop. More details of the experimental set up, and test section are discussed in Ref [18, 19].

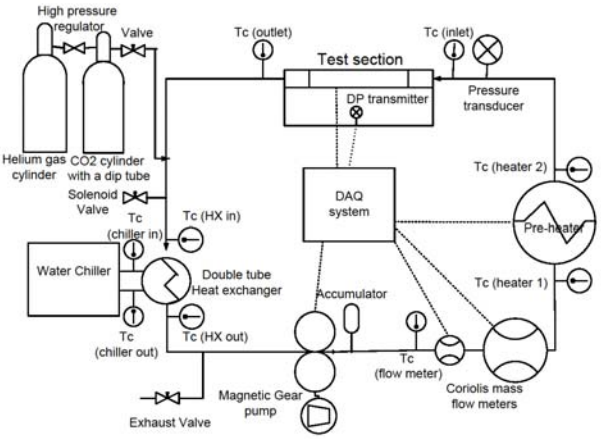

Figure 1. Schematic of experimental facility

Experimental conditions and procedure

The experiments were performed with a change of the inlet pressure, mass flow rate, and wall heat flux at different inlet temperatures in order to investigate effects of these parameters on heat transfer performance. The corresponding Reynolds number based on the inlet condition varied from 20,000 to 50,000. During the test, all parameters such as temperatures, mass flow rate, and heating power were monitored and controlled by Labview DAQ system [18, 19]. Table 1 summarizes the experimental conditions.

* Correspondence Author: reza.sadr@qatar.tamu.edu

Table 1 Range of all experimental conditions.

Inlet temp. [°C]	q" [kW/m^2]	P [bar]	$\dot{m}$ [kg/s]
22, 24, 26, 28	31, 49, 64	75, 80, 85, 90	0.011, 0.014, 0.017

DATA REDUCTION AND UNCERTAINTY ANALYZE

The inlet and outlet temperatures, surface wall temperatures, mass flow rate, and inlet pressure were measured as key experimental parameters to obtain the heat transfer coefficient at each location. Data reduction procedure is briefly described in this section.

Heat transfer coefficient is obtained by using the following procedure. First, the total surface heat flux into the test section is calculated using enthalpy at the inlet and outlet as [19]:

$$q" = \dot{m}(i_{out} - i_{in})/A_t \,, \qquad (1)$$

where A_t is the total area of the outer surface of the test section. The enthalpy at the inlet and outlet were obtained from NIST thermal database using the measured temperatures [20]. In this study, assuming steady state conditions, the semi local averaged convective heat transfer q_c, and fluid bulk temperature T_b at the each location were computed by using energy balance relations including conduction in the axial direction and assuming constant heat flux from electrical heaters [18, 19]. Conduction heat transfer in the direction of the flow in the wall may not be neglected since the test section wall temperature varies due to the change in the fluid bulk temperature and wall heat transfer convection. The fluid bulk temperature and semi-local heat transfer coefficient were obtained by solving following two equations [18, 20]:

$$kA_{tu}\frac{T_{i-1}-T_i}{\Delta l} + kA_{tu}\frac{T_{i+1}-T_i}{\Delta l} + q"_c A_{out} + \bar{h}A_{in}(\bar{T}_b - \bar{T}_w) = 0, \qquad (2)$$

$$T_{b+1} = T_b + q"_c \pi D/(\dot{m}c_p)L \,. \qquad (3)$$

More details are described in Ref [18].

The experimental uncertainty in the measurement is mainly due to the uncertainties in the measured pressure, mass flow rate, and temperatures. In order to improve the accuracy of the measurements, thermocouple probes were accurately calibrated using a NIST standard RTD probe and constant temperature bath and the uncertainties were established before installation. The accuracies of the thermocouple probes used to measure inlet and outlet bulk temperatures were ±0.15 °C while the accuracies of the measured wall surface temperatures were ±0.2 °C, for the temperature range tested in the present study. The total uncertainties in the measurements of the semi-local heat transfer coefficient, and Nusselt number were estimated to be 10%, and 15%, respectively. Note that all thermal properties of carbon dioxide used in this work are obtained at local fluid temperature and pressure from NIST thermal database [20].

RESULTS AND DISCUSSION

In this section, the effects of wall heat flux, mass flow rate, and inlet pressure on the heat transfer characteristics are briefly discussed. Nusselt numbers obtained from the current experiments were then compared with the Dittus-Boelter type correlations suggested in the literature for modeling the heat transfer in pseudocritical flow.

Heat transfer measurements

Semi local heat transfer coefficients along the tube were obtained from the measurements using energy balance in each section of the tube [18]. The distribution of the semi-local heat transfer coefficient for the case 1 is plotted as a function of the distance from the inlet normalized by the tube length in figure 2a to c. Note that for all the cases, first two and last one measuring points are eliminated due to possible errors associated with the entrance and end effects. Table 2 shows the different test cases shown in Figures 2 to 5.

Table 2 Range of experimental parameters in the current test campaign at T_{in}=24°C.

Case	q" [kW/m^2]	$\dot{m}$ [kg/s]	P [bar]
1	31, 49, 64	0.011	80
2	49	0.011,0.014,0.017	80
3	49	0.011	75, 80, 85, 90

Figure 2a generally indicates that the heat transfer coefficient decreases as the wall heat flux increases. For wall heat flux of 31 kW/m^2 the heat transfer coefficient improves and plateau from x/L=0.3 to 0.5 where the bulk temperature reach close to the pseudocritical temperature. The heat transfer coefficient then deteriorates after x/L=0.5. This highest point of heat transfer coefficient is shifted upstream with an increase in wall heat fluxes that is an indication of the heat transfer enhancement near the pseudocritical region. The heat transfer coefficient continues to deteriorate throughout the test section for the heat flux cases of 49 and 64 kW/m^2. Interestingly this deterioration reaches its peak for the case of 63 kW/m^2 around x/L=0.75.

As expected, Figure 2b shows that the heat transfer coefficient generally increases with increasing the mass flow rate as higher mass flow rate reduces the wall temperature. However, a local peak heat transfer coefficient is observed at higher mass flow rates that are an indication of heat transfer enhancement in the middle of the tube corresponding to pseudocritical region. After heat transfer coefficient reaches local peak (x/l=0.5), it deteriorates sharply. There is no local peak observed in the tube for the mass flow rate of 0.011kg/s.

Figure 2c indicates that, for the heat flux of 49 kW/m^2, the trends of heat transfer coefficient along the test section are similar to each other with a clear enhancement for the case of 75 that is closest case to the critical point of CO_2 in this work.

* Correspondence Author: reza.sadr@qatar.tamu.edu

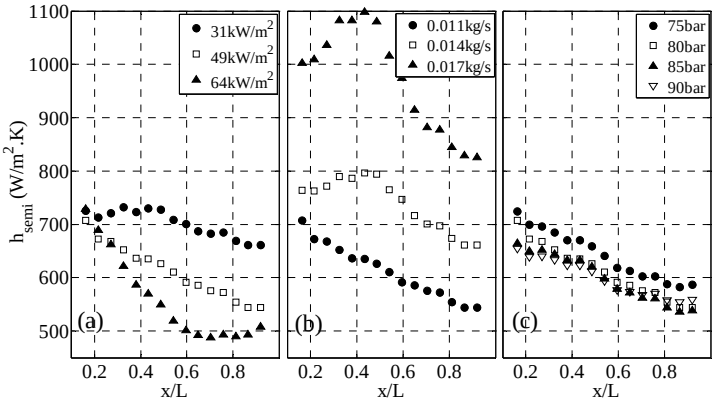

Figure 2. Variation of semi-local heat transfer coefficients along the tube

Brief review of empirical correlations

Due to the difficulty associated with the drastic thermal property variation in the pseudocritical region, comprehensive models for predicting convection heat transfer for turbulent flow have not been developed yet. The experimental results are compared with a few correlations chosen among several suggested correlations in the literature. The measured Nusselt number in this work is compared with those calculated using Dittus-Boelter type correlations.

Initially the experimental results are compared with the results of the Dittus-Boelter correlation. Dittus-Boelter is used as the basis to study the flow field in a fully developed turbulent pipe flow in single phase with no major property variation. This comparison can be used as a reference for assessing the heat transfer enhancement, or deterioration, in both heating and cooling conditions in a pipe in pseudocritical region [15].

Dittus-Boelter correlation provides an estimation of the local Nusselt number with the assumption of constant property in the fluid [21],

$$Nu_b = 0.023 Re_b^{0.8} Pr_b^{0.4}. \quad (4)$$

Later modifications were proposed to improve Equation 4 for super critical flows by including additional terms in Equation 4 to account for property variations. Our previous study [26] showed the effect of the buoyancy could not be neglected in the present experimental conditions. The buoyancy force is mainly generated by the density variation between the bulk and pipe near wall condition.

Ornatsky et al. improved Shitsman's empirical correlation for forced convection inside tubes at supercritical pressures [22]:

$$Nu_b = 0.023 Re_b^{0.8} Pr_{min}^{0.8} \left(\frac{\rho_w}{\rho_b}\right)^{0.3}. \quad (5)$$

Pr_{min} is the minimum value of Pr_w or Pr_b.

Bishop et al. [23] performed convective heat transfer measurements using supercritical water flowing inside vertical tubes and then developed the following correlation for small tubes with 2.5–5.1 mm inner diameters. The correlation includes the inlet effect in the last term of the equation:

$$Nu_b = 0.0069 Re_b^{0.9} \overline{Pr_b^{0.66}} \left(\frac{\rho_w}{\rho_b}\right)_x^{0.43} \left(1 + 2.4\frac{D}{x}\right). \quad (6)$$

Jackson and Hall [25] further improved Krasnoshchekov's [24] for forced convective heat transfer in both supercritical water and CO_2. They use a Dittus-Boelter type of equation for a constant property for forced convection in conjunction with the terms of the property changes between fluid bulk and near wall regions. Buoyancy effects are not directly considered in this correlation but exponents associated with specific heat varies with temperatures in the flow. Jackson and Hall's correlation represented as:

$$Nu = 0.0183 Re_b^{0.82} Pr_b^{0.5} \left(\frac{\rho_w}{\rho_b}\right)^{0.3} \left(\frac{\overline{c_p}}{c_{pb}}\right)^n, \quad (7)$$

where the exponent n is given by following:

$$n = 0.4, \qquad \frac{T_b}{T_{pc}} < \frac{T_w}{T_{pc}} \le 1 \; or \; 1.2 \le \frac{T_b}{T_{pc}} < \frac{T_w}{T_{pc}}$$

$$n = 0.4 + 0.2\left(\frac{T_w}{T_{pc}} - 1\right), \qquad \frac{T_b}{T_{pc}} \le 1 < \frac{T_w}{T_{pc}}$$

$$n = 0.4 + 0.2\left(\frac{T_w}{T_{pc}} - 1\right)\left[1 - 5\left(\frac{T_b}{T_{pc}} - 1\right)\right],$$

$$1 < \frac{T_b}{T_{pc}} < 1.2 \; and \; \frac{T_b}{T_{pc}} < \frac{T_w}{T_{pc}}. \quad (8)$$

Note that $\overline{Pr}$ is averaged Prandtl number which is defined as $\overline{Pr} = \frac{\mu_b \overline{c_p}}{k_b}$ and $\bar{c}_p$ is defined as an averaged value of specific heats at the wall and bulk:

$\bar{c}_p = \frac{i_w - i_b}{T_w - T_b}$.

This correlation was valid within the following ranges:

$8\times10^4 < Re_b < 5\times10^5$,

$0.85 < Pr < 65$,

$0.09 < (\rho_w/\rho_b) < 1.0$,

$0.02 < \bar{c}_p/c_{pb} < 4.0$,

$0.9 < T_w/T_{pc} < 2.5$, and

$46 kW/m^2 < q < 2.6 MW/m^2$.

The results of the comparisons with the experimental data are shown in the next section.

Results of comparison

Comparison with correlation without property change:

Figure 3 shows comparison of the experimental data in this work with Dittus-Boelter results obtained from Equation (4). As expected, the Dittus-Boelter correlation enormously over-predicts the normalized convection heat transfer coefficient. However, the difference between the correlation and experimental data narrows down as the inlet pressure increases in general and for x/L > 0.6. The location of x/L > 0.6 corresponds to the region where the fluid bulk temperature became far from its pseudocritical temperature ($T_b >> T_{pc}$). Since the property variation between near wall and bulk becomes small, it can be better approximated by constant property.

* Correspondence Author: reza.sadr@qatar.tamu.edu

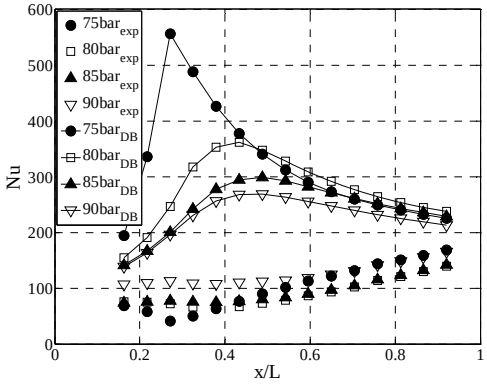

Figure 3. Typical for comparison of the experimental data with that of Dittus-Boelter prediction for case 3.

Comparison with correlation with property change:

Figure 4 presents detail comparison of the experimental data with correlations 5, 6, and 7 for case 1 in table 1. The correlation by Ornatsky, Nu_{OR}, shows much better agreement with that of Dittus-Boelter, but it underestimates Nu. Furthermore, it does not capture the variation for the pseudocritical flow inside the tube as it shows an almost linear increase along the test section. The difference between the correlation and the data becomes larger as the mass flow rate is increased. The outstanding capability of the Bishop's correlation (Nu_{BI}) for prediction of Nu is seen in Figure 4a and b as it successfully catches the trends for lower heat flux. However, the predicted values from Bishop's correlation are slightly under-predicted for x/L<0.5, Figure 4c. Although the correlation by Jackson-Hall (Nu_{JH}) showed similar trends to that of the experiment, it underestimates Nu for x/L<0.7 at the lower wall heat fluxes and for the highest wall heat flux cases; those regions correspond to the pseudocritical region in the flow.

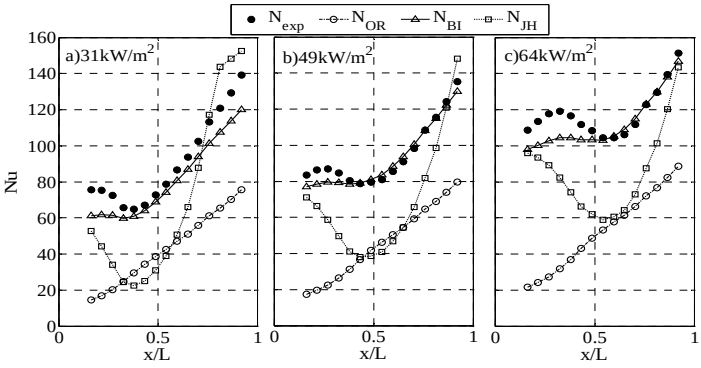

Figure 4. Comparison of the experimental data with correlations 5, 6, and 7 for case 1.

Figure 5 indicates detail comparison of the experimental data with correlations for case 2 in table 1. The prediction made by Ornatsky again shows a simple linear increase along the pipe and underestimates the experimental Nu. The outstanding capability of the Bishop's correlation (Nu_{BI}) is again evident in Figures 5a and b. The Bishop's correlation could follow the same trend of the experimental data for the lower mass flow rates, however it slightly underestimates the experimental data for the mass flow rate of 0.017kg/s. Jackson-Hall correlation fails to predict the current experimental data. Especially, the correlation performs poorly when the bulk temperature is near the pseudocritical region for all the case. Also, the prediction becomes worse as the mass flow rate increases. However, the prediction of Jackson-Hall correlation approaches the experimental data when the bulk temperature is far from the pseudocritical region.

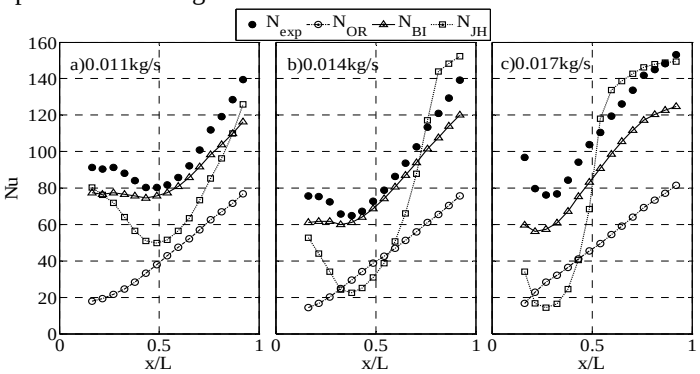

Figure 5. Comparison of the experimental data with correlations 5, 6, and 7 for case 2.

Figure 6 shows detailed comparison of the experimental data with correlations 5, 6, and 7 for case 3 in Table 1. Although Nu prediction by the correlation of Ornatsky shows a much better agreement with the measurements than that of Dittus-Boelter, it underestimates Nu with an almost linear increase along the test section; furthermore, it does not catch the experimental trend especially in the pseudocritical region. The superior prediction capability of Bishop's correlation is seen in figure 6a to c. It successfully catches the experimental trend for the lower heat flux case. However, the predicted values from Bishop's correlation are slightly under-predicted for lower pressures, Figures 6a to c at x/L > 0.6, and along the entire test section for 90 bar pressure, Figure 6d. Jackson-Hall underestimated experimental data along all the test section for all the experimental pressures.

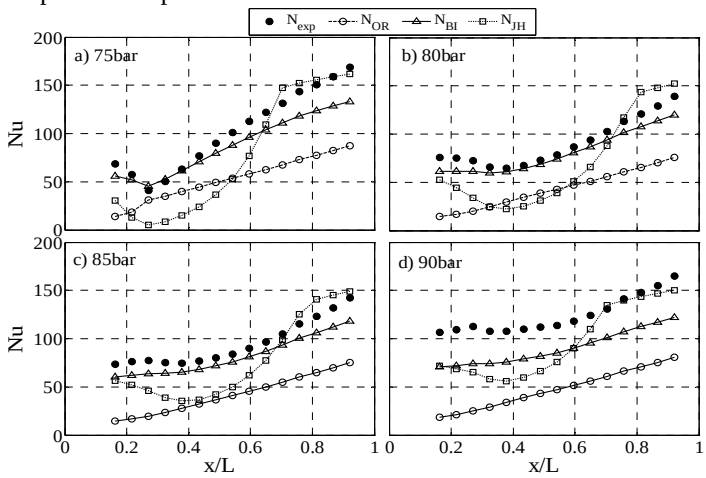

Figure 6. Comparison of the experimental data with correlations 5, 6, and 7 for case 3.

Two parameters of mean error and its standard deviation of the calculated Nusselt numbers from the correlations studied in this work may be used to evaluate their performance compared

* Correspondence Author: reza.sadr@qatar.tamu.edu

to the experimental data [12]. In general it is evident the Dittus-Boelter correlation performs very poorly for the flow field and experimental conditions presented in this work. The mean error between this correlation and data was 245.5%. This correlation captures only 1.64% of the data within the error of ±30%. The standard deviation of the correlation against the experimental data was 360.1%.

Figure 7 shows a comparison between the predictions by the three discussed correlations for SCO_2 (Equations 5, 6, and 7) with data for all the present experimental conditions which were more than 2700 data points in total. Overall, the Ornatsky correlation (Equation 5) also shows poor agreement with the measurements. This result indicates that the mean error between this correlation and data is 53.0%. The standard deviation of the correlation against the experimental data was 55.1%. The correlation was under-predicted in most of the cases capturing only 5.8% of the data within the error band of ±30%.

Bishop's correlation (Equation 6) showed the best agreement with the current experimental data. This correlation predicted the semi local Nusselt number best in terms of the mean error which is 15.1%. The standard deviation of the correlation against the experimental data is 19.2%. Bishop's correlation captured 90.7% of the data within the error band of ±30%.

Jackson-Hall (Equation 7) performed reasonably well in the current experiments. The mean error between this correlation and data is 29.7%. This correlation captured 58.0% of the data within the error of ±30%. Compared to the Bishop's correlation the results of Jackson and Hall are widely spread. The standard deviation of the correlation against the experimental data is 38%.

Table 3 shows the summarized results from the current experiments. Overall, the correlations employed averaged Prandtl number, $\overline{Pr}$, and density ratio between the wall and bulk give adequate prediction for the present data.

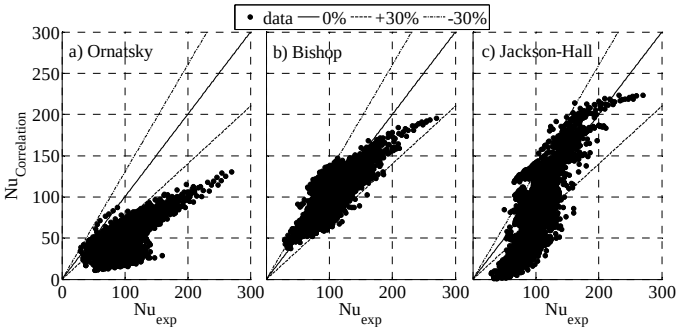

Figure 7 Overall comparisons of the experimental data with correlations.

Table 3 Summarized results

Correlations	Mean Error (%)	Captured (%)	STD
Dittus-Boelter	245.5	1.64	360.1
Ornatsky	53.0	5.8	55.1
Bishop	15.1	90.7	19.2
Jackson-Hall	29.7	58.0	38

From the above discussion, it can be concluded that the Bishop's correlation gives the best prediction for the current experimental data within an acceptable range of errors. It is worth mentioning that the tube diameter used to develop Bishop's correlation is different from that used in the current study. This may be a reason for the lower performance of the Bishop correlation in this work indicating the influence of tube diameter on performance of the suggested correlations.

CONCLUSION

Experimental investigations for the forced convection heat transfer to SCO_2 flowing in a horizontal tube heated at a constant heat fluxes were carried out with various inlet conditions in MSTF lab in order to properly understand the thermal and dynamic characteristics of these flows. Forced convective heat transfer coefficients were obtained under several combinations of wall and bulk fluid temperatures near pseudocritical temperature. Heat transfer enhancement and hindrance in the test section was observed at some operating conditions.

The experimental dataset was analyzed by comparing measured semi-local Nusselt numbers with the four Dittus-Boelter type correlations. The comparisons indicate the correlation without property variation did not predict correctly and over-predicted. The comparisons also indicated the correlation with averaged Prandtl number is better agreement than using Prandtl number at the fluid bulk. In general, the correlation of Bishop's correlation appears to closely follow the trend of the experimental data. The correlation of Bishop was in best agreement with the current experimental data than the other correlations. A new heat transfer correlation will be developed based on the combination of Bishop's correlation and experimental data in the future work.

ACKNOWLEDGMENTS

This publication was made possible by NPRP grant # 08-494-193 and 09-1183-2-461 from the Qatar National Research Fund (a member of Qatar Foundation). The statements made herein are solely the responsibility of the authors. The authors wish to thank Dr. Devesh Ranjan at Texas A&M for his insight and constructive advice in this project.

REFERENCES

[1] U.S. Energy Information Administration, 2013, "International Energy Outlook 2013 with Projections to 2040," http://www.eia.gov/forecasts/ieo/, report No. DOE/EIA-0484(2013).

[2] Dostal, V., 2004, "A supercritical carbon dioxide cycle for next generation nuclear reactor," PhD thesis, MIT.

[3] Wright, S. A. Radel, R. F. and Fuller, R., 2010, "Engineering performance of supercritical CO_2 Brayton cycles," Proceedings of ICAPP 10, June 13-17, San Diego, CA, USA.

[4] Li, H. Kruizenga, A. Anderson, M. Corradini, M. Luo, Y. Wang, H. and Li, H., 2011, "Development of a new forced convection heat transfer correlation for CO_2 in both heating

* Correspondence Author: reza.sadr@qatar.tamu.edu

and cooling modes at supercritical pressures," Int. Journal of Thermal Sciences, 50, 2430-2442.
[5] Conboy, T. Wright, S. Pasch, J. Fleming, D. and Rochau, G., 2012, "Performance Characteristics of an Operating Supercritical CO_2 Brayton Cycle," Journal of Engineering for Gas Turbines and Power, 134 **(**11**)**, 111703-1.
[6] Dostal, V. Hejzlar, P. and Driscoll, M. J., 2006, "The Supercritical Carbon Dioxide Power Cycle: Comparison to Other Advanced Power Cycles," Nuclear Technology, 154 **(**3**)**, 283–301.
[7] Wright, S. A. Conboy, T. M. Parma, E. J. Lewis, T. G. Rochau, G. A. and Suo-Anttila, A. J., 2011, "Summary of the Sandia Supercritical CO_2 Development Program. S CO_2 Power Cycle Symposium," May 24-25, Boulder, Colorado, USA.
[8] Carles, P., "A brief review of the thermopyhical properties of supercritical fluids," The Journal of Supercritical Fluids, 53 (1), 2-11.
[9] Liao, S. M. and Zhao, T. S., 2002, "An experimental investigation of convection heat transfer to supercritical carbon dioxide in miniature tubes," International Journal of Heat and Mass Transfer, Vol. 45 (25), pp. 5025-5034.
[10] Bruch, A., Bontemps, A. and Colasson, S., 2009, "Experimental investigation of heat transfer of supercritical carbon dioxide flowing in a cooled vertical tube," International Journal of Heat and Mass Transfer," 52 (11-12), pp. 2589-2598.
[11] Kim, D. E. and Kim, M., 2011, "Experimental investigation of heat transfer in vertical upward and downward supercritical CO_2 flow in a circular tube," International Journal of Heat and Fluid Flow, 32 (1), pp. 176-191.
[12] Bae, Y. Y., Kim, H. Y. and Kang, D. J., 2010, "Forced and mixed convection heat transfer to supercritical CO_2 vertically flowing in a uniformly-heated circular tube," Experimental Thermal and Fluid Science, 34 (8), pp. 1295-1308.
[13] Li, Z. H., Jiang, P. X., Zhao, C. R. and Zhang, Y., 2010, "Experimental investigation of convection heat transfer of CO_2 at supercritical pressures in a vertical circular tube," Experimental Thermal and Fluid Science, 34 (8). pp. 1162-1171.
[14] Kim, H, Kim, H. Y., Song, J. H. and Bae, Y. Y., 2008, "Heat transfer to supercritical pressure carbon dioxide flowing upward through tubes and a narrow annulus passage," Progress in Nuclear Energy, 50, pp. 518-525.
[15] Lin, W., Du. Z. and Gu, A., 2012, "Analysis on heat transfer correlations of supercritical CO_2 cooled in horizontal circular tubes," Heat and Mass Transfer, 48, pp. 705-711.
[16] Pioro, I. L. and Duffey, R. B., 2007, "Heat transfer and hydraulic resistance at supercritical pressures in power-engineering applications," ASME.
[17] Yoo, J. Y., 2013, "The Turbulent Flows of Supercritical Fluids with Heat transfer," Annual Reviews of Fluid Mechanics, 45, pp. 495-525.
[18] Tanimizu, K. and Sadr, R., 2012, "Experimental Investigation of Heat transfer Characteristics of Pseudocritical Carbon Dioxide in a circular horizontal tube," ASME SUMMER Heat Transfer Conference, July 8-12, Puerto Rico, Paper No. HT2012-58331.
[19] Sadr, R., Kannaiyan, K., Kanjirakat, A. and Tanimizu, K., 2013, "Macro- to microscale thermo-fluids research in energy efficient systems," In Excellence and impact of research at Texas A&M at Qatar, Ed. Weichold, M., Hall, K., Masad, E., and Leonard, C., Qatar, Qsience.
[20] NIST Standard Reference Database 23 version 9.0 (REFPROP).
[21] Incropera, F.P. Dewitt, D.P. Bergman, T.L. and Lavine, A.S., 2007, "Fundamentals of Heat and Mass Transfer," John Wiley & Sons, New Jersey.
[22] Ornatsky, A.P., Glushchenko, L.P., Siomin, E.T., et al., 1970, "The research of temperature conditions of small diameter parallel tubes cooled by water under supercritical pressures," In: Proceedings of the Fourth International Heat Transfer Conference, Paris-Versailles, France, vol. VI. Paper B 8.11, Elsevier, Amsterdam.
[23] Bishop, A.A., Sandberg, R.O. and Tong, L.S., 1964, "Forced convection heat transfer to water at near-critical temperatures and supercritical pressures," Report WCAP-2056, Part IV, November, Westinghouse Electric Corp., Pittsburgh, USA.
[24] Krasnoshchekov, E.A. and Protopopov, V.S., 1960, "About heat transfer in flow of carbon dioxide and water at supercritical region of state parameters, (In Russian)," Thermal Eng. 10, 94.
[25] Jackson, J. D. and Hall, W. B., 1979, "Influences of buoyancy on heat transfer to fluids flowing in vertical tubes under turbulent conditions," in: Kakac, S., and Spalding, D. B. (Eds), Turbulent Forced Convection in Channels and Bundles, 2, Hemisphere Publishing Corp., New York, USA, pp. 613-640.
[26] Tanimizu, K. and Sadr, R., 2013, "Experimental Investigation of buoyancy effect on turbulent heat transfer of S-CO_2 flowing in a horizontal tube," submitted to Journal of heat transfer, No. HT-13-1252.

* Correspondence Author: reza.sadr@qatar.tamu.edu